

1  
2  
3  
4  
5  
6  
7  
8  
9  
10  
11  
12  
13  
14  
15  
16  
17  
18  
19  
20  
21  
22  
23  
24  
25

**Microflowmeter-tension disc infiltrometer: Part II. Hydraulic properties  
estimation from transient infiltration rate analysis**

**David Moret-Fernández<sup>a\*</sup>, Borja Latorre<sup>a</sup>, César González-Cebollada<sup>b</sup>**

<sup>a</sup> *Departamento de Suelo y Agua Estación Experimental de Aula Dei Consejo Superior de Investigaciones Científicas (CSIC). PO Box 202, 50080, Zaragoza, Spain.*

<sup>b</sup> *Área de Mecánica de Fluidos. Escuela Politécnica Superior de Huesca - Universidad de Zaragoza. Carretera de Cuarte s/n. 22071, Huesca, Spain.*

\* Corresponding author.

*Telf:* +34 976 71 61 40

*Fax:* +34 976 71 61 45

*E-mail address:* [david@eead.csic.es](mailto:david@eead.csic.es)

1  
2  
3  
4  
5  
6  
7  
8  
9  
10  
11  
12  
13  
14  
15  
16  
17  
18  
19  
20  
21  
22  
23

**ABSTRACT**

Measurements of soil sorptivity ( $S_0$ ) and hydraulic conductivity ( $K_0$ ) are of paramount importance for many soil-related studies involving disciplines such as agriculture, forestry and hydrology. In the last two decades, the disc infiltrometer has become a very popular instrument for estimations of soil hydraulic properties. The previous paper in this series presented a new design of disc infiltrometer that directly estimates the transient flow of infiltration rate curves. The objective of this paper is to present a simple procedure for estimating  $K_0$  and  $S_0$  from the linearization of the transient infiltration rate curve with respect to the inverse of the square root of time (IRC). The technique was tested in the laboratory on 1D sand columns and 1D and 3D 2-mm sieved loam soil columns and validated under field conditions on three different soil surfaces. The estimated  $K_0$  and  $S_0$  were subsequently compared to the corresponding values calculated with the Vandervaere et al. (2000) technique, which calculates the soil hydraulic parameters from the linearization of the differential cumulative infiltration curve with respect to the square root of time (DCI). The results showed that the IRC method, with more significant linearized models and higher values of the coefficient of determination, allows more accurate estimation of  $K_0$  and  $S_0$  than the DCI technique. Field experiments demonstrate that the IRC procedure also makes it possible to detect and eliminate the effect of the sand contact layer commonly used in the disc infiltrometry technique. Comparison between the measured and the modelled cumulative infiltration curves for the  $K_0$  and  $S_0$  values estimated by the DCI and IRC methods in all the 1D and 3D laboratory experiments and field measurements shows that the IRC technique allowed better fittings between measured and modelled cumulative infiltration curves, which indicates better estimations of the soil hydraulic properties.

1 *Key words:* Sorptivity; Hydraulic Conductivity; Cumulative Infiltration.

2

### 3 **1. INTRODUCTION**

4 Infiltration-based methods are recognized as valuable tools for studying hydraulic and transport  
5 soil properties. Over the last two decades, the tension disc infiltrometer has become a popular  
6 infiltration method for estimating soil hydraulic characteristics because of the relatively rapid and  
7 portable nature of this technique and its easy *in-situ* applicability. An important advantage of this  
8 technique over laboratory methods is that it is performed *in situ*, which allows exploration of the  
9 dependence of hydraulic properties on soil structure (Vandervaere et al., 2000). This instrument  
10 originally consisted of a base disc jointed to a graduated water-supply reservoir and a bubble tower to  
11 impose a negative pressure head ( $\psi$ ) at the base disc (Perroux and White, 1988). The soil hydraulic  
12 properties are commonly estimated from an analysis of the cumulative infiltration curve, which can  
13 be monitored by visually noting the water-level drop in the reservoir tower or by automated systems  
14 such as pressure transducers (Ankeny et al., 1988; Casey and Derby, 2002) or the TDR technique  
15 (Moret et al., 2004). However, recent designs of disc infiltrometers, which directly estimate the water  
16 infiltration rate using a microflowmeter inserted between the water reservoir and the disc base  
17 (Moret-Fernández and González, 2009; Moret-Fernández et al., 2011; Moret-Fernández et al., 2012),  
18 suggest that, unlike the classical disc infiltrometers, soil hydraulic properties can be directly  
19 calculated from analysis of the infiltration rate curves.

20 Various techniques are so far available for inferring hydraulic properties from the measured  
21 infiltration curves. The earliest infiltrometry methods are based on the analysis of the steady-state  
22 water flow. Steady-state flow theory, which is based on the simple Wooding equation (1968), has  
23 been widely used and compared during the last few decades (Perroux and White, 1988; White et al.,  
24 1992; Logsdon and Jaynes, 1993). Estimation of the soil hydraulic properties using the Wooding  
25 equation (1968) can be achieved by the multiple disc approach (Smettem and Clothier, 1989) or the

1 multiple head approach (Ankeny et al., 1991; Reynolds and Elrick, 1991). However, the assumption  
2 of homogeneous isotropic soil with uniform initial water content required by the Wooding equation  
3 (1968), together with the length of time needed to achieve the steady-state water flow, may restrict  
4 their use in field conditions (Vandervaere et al., 2000).

5 Determination of soil hydraulic properties can alternatively be carried out from an analysis of the  
6 transient water flow. This method, which means shorter experiments and smaller sampled volumes of  
7 soil, is obviously in better agreement with assumptions of homogeneity and initial water uniformity  
8 (Angulo-Jaramillo et al., 2000). Valiantzas (2010), proposed a two-parameter equation which is a  
9 specific solution that is approximately located at the middle of the domain of real soils defined by  
10 two “limiting” behaviour soils. Other expressions used to estimate the soil hydraulic parameters from  
11 the transient flow (Warrick and Lomen, 1976; Warrick, 1992; Zhang, 1997; Smettem et al., 1994)  
12 have in common the two-term equation proposed by Philip (1957) for three-dimensional cumulative  
13 infiltration ( $I$ )

$$14 \quad I = S\sqrt{t} + At \quad (1)$$

15 where  $t$  is time (T),  $S$  is the capillary sorptivity ( $L T^{-1/2}$ ) and  $A$  is a parameter dependent on the soil  
16 hydraulic conductivity ( $K$ ) ( $L T^{-1}$ ). Using previous work by Turner and Parlange (1974) and Smettem  
17 et al. (1994), Haverkamp et al. (1994) proposed a physically based expression similar to Eq. (1), valid  
18 for a short to medium time. Vandervaere et al. (2000) suggested and compared several methods to  
19 analyse the Haverkamp et al. (1994) equation for disk infiltrometer measurements and concluded that  
20 the linear fitting technique consisting of a differentiation of the cumulative infiltration data with  
21 respect to the square root of time allowed the best estimations of soil hydraulic properties. These  
22 authors suggested that direct non-linear fitting of the cumulative infiltration or infiltration flux was  
23 likely to lead to unacceptable errors, either because of difficulties in dealing with the non-uniqueness  
24 of the solution or the influence of the contact sand layer.

1 Determination of the soil hydraulic properties can also be made by inverse modelling the entire  
2 experimental cumulative infiltration data; however the analysis of numerically generated data for one  
3 tension experiment demonstrated that the cumulative infiltration curve by itself does not contain  
4 enough information to provide a unique inverse solution (Simunek and van Genuchten, 1996 and  
5 1997). An infinite number of combinations of the saturated hydraulic conductivity can be obtained in  
6 almost identical infiltration curves (Vandervaere et al., 2000). The one- and three-dimensional  
7 infiltration curves can be also be obtained from a quasi-exact analytical solution of the Richard's  
8 equation (Parlange et al., 1982; Haverkamp et al., 1994).

9 The objective of this paper is to present a new method of estimating soil hydraulic properties from  
10 direct analysis of the infiltration rate curve measured with the new infiltrometer design described in  
11 the previous paper of this series (e.g. Moret-Fernandez et al., 2011). This method calculates the soil  
12 hydraulic parameters from the linearization of the infiltration rate curve with respect to the inverse of  
13 the square root of time. The new procedure, which was tested in a laboratory on 1D and 3D soil  
14 columns and validated in field infiltration experiments, was subsequently compared with the  
15 Vandervaere et al. (2000) method commonly used in standard disc infiltrometers. The cumulative  
16 infiltration measured with the disc infiltrometer was finally compared with the corresponding  
17 modelled curves obtained by applying the estimated hydraulic properties to the quasi-exact analytical  
18 form of the 1D (Parlange et al., 1982) and 3D (Haverkamp et al., 1994) cumulative infiltration  
19 curves.

20

## 21 **2. THEORY**

22 The cumulative infiltration per unit of area ( $I$ ) (L) can be expressed as (Smettem et al., 1994)

23 
$$I_{3D} = I_{1D} + \frac{\gamma S^2}{R_D(\theta_0 - \theta_n)} t \quad (2)$$

1 where the subscripts 3D and 1D refer to axisymmetric three-dimensional and one-dimensional  
 2 processes respectively;  $R_D$  (L) is the radius of the disc;  $\theta_0$  and  $\theta_n$  are the final and initial volumetric  
 3 water content ( $L^3 L^{-3}$ ), respectively; and  $\gamma$  is the proportionality constant corrected for the use of  
 4 simplified wetting front, sorptivity, and gravity assumptions, the value of which can be approximated  
 5 to 0.75 (Haverkamp et al., 1994; Angulo-Jaramillo et al., 2000).

6 For unsaturated conditions, the one-dimensional infiltration curve can be expressed in the quasi-  
 7 exact analytical form (Parlange et al., 1982)

$$8 \quad \frac{2(K_0 - K_n)^2}{S_0^2} t = \frac{2}{1 - \beta} \frac{(K_0 - K_n)(I_{1D} - K_n t)}{S_0^2} -$$

$$9 \quad \frac{1}{1 - \beta} \cdot \ln \left\{ \exp(2\beta(K_0 - K_n)(I_{1D} - K_n t) / S_0^2) + \beta - 1 \right\} (\beta)^{-1} \quad (3)$$

10 where  $S_0$  is the sorptivity for  $\theta_0$ ;  $K_0$  and  $K_n$  are the hydraulic conductivity values corresponding to  $\theta_0$   
 11 and  $\theta_n$ , respectively; and  $\beta$  is a shape constant constrained to  $0 < \beta < 1$  (Haverkamp et al., 1994) for  
 12 which an average value of 0.6 is taken (Angulo-Jaramillo et al., 2000). Substituting Eq. (3) into Eq.  
 13 (2), Haverkamp et al. (1994) found that the three-dimensional infiltration equation yields

$$14 \quad \frac{2(K_0 - K_n)^2}{S_0^2} t = \frac{2}{1 - \beta} \frac{K_0 - K_n}{S_0^2} \cdot \left\{ I_{3D} - K_n t - \left[ \gamma S_0^2 / R_D (\theta_0 - \theta_n) \right] t \right\}$$

$$15 \quad - \frac{1}{1 - \beta} \cdot \ln \left\{ \exp \left[ 2\beta(K_0 - K_n) / S_0^2 \right] \left[ I_{3D} - K_n t - \left( \gamma S_0^2 / R_D (\theta_0 - \theta_n) \right) t \right] + \beta - 1 \right\} (\beta)^{-1} \quad (4)$$

16 In spite of their relative complexity, Eqs. (3) and (4) have the advantage of being valid for the entire  
 17 time range from  $t = 0$  to  $t = \infty$ . However, taking into account that infiltrometer experiments do not  
 18 require very long time ranges of application, Haverkamp et al. (1994) established that for short to  
 19 medium time and assuming  $K_n \rightarrow 0$ , the 3D cumulative infiltration curve can be defined with the  
 20 simplified but highly accurate equation

$$21 \quad I_{3D} = S_0 \sqrt{t} + \left[ \frac{2 - \beta}{3} K_0 + \frac{\gamma S_0^2}{R_D (\theta_n - \theta_0)} \right] t \quad (5)$$

1 The first term of the right-hand side corresponds to the vertical capillary flow and dominates the  
 2 infiltration during its early stages. The second term corresponds to the gravity-driven vertical flow,  
 3 and the third term represents the lateral capillary flow component (Angulo-Jaramillo et al., 2000).

4 Substituting Eq. (5) into Eq. (2), the form for one-dimensional infiltration conditions reduces to

$$5 \quad I_{1D} = S_0 \sqrt{t} + \left[ \frac{2-\beta}{3} K_0 \right] t \quad (6)$$

6 Eqs. (5) and (6) can be simplified to a two-term expression (Vandervaere et al., 2000) according to

$$7 \quad I = C_1 \sqrt{t} + C_2 t \quad (7)$$

8 where

$$9 \quad C_1 = S_0 \quad (8)$$

10 and

$$11 \quad C_2 = \frac{2-\beta}{3} K_0 + \frac{\gamma C_1^2}{R_D (\theta_n - \theta_0)} \quad (9)$$

12 for the three-dimensional conditions, or

$$13 \quad C_2 = \frac{2-\beta}{3} K_0 \quad (10)$$

14 if a one-dimensional infiltration process is under consideration.

15 The time derivative of Eq. (7), which represents the infiltration rate curve ( $q$ ), is expressed as

$$16 \quad q = \frac{C_1}{2\sqrt{t}} + C_2 \quad (11)$$

17 Four different methods of inferring  $S_0$  and  $K_0$  values from  $C_1$  and  $C_2$  have been described in  
 18 Vandervaere et al. (2000). These authors concluded that the linear fitting technique consisting of a  
 19 differentiation of the cumulative infiltration data with respect to the square root of time (DCI), and  
 20 expressed as

$$21 \quad \frac{dI}{d\sqrt{t}} = C_1 + 2C_2 \sqrt{t} \quad (12)$$

1 was the only method that allowed visual checking of the validity and range of applicability of the  
2 two-term equation. This method has been successfully used to reveal and eliminate the influence of  
3 the sand contact layer on the first steps of the cumulative infiltration curve, whose effects produce  
4 important errors in the estimations of the soil hydraulic properties (Vandervaere et al., 2000).

5

6

## 7 **2. MATERIAL AND METHODS**

### 8 *2.1. Column experiments*

9 The method proposed here estimates  $S_0$  and  $K_0$  from the  $C_2$  and  $C_1$  parameters (Eqs. 8, 9 and 10),  
10 which are obtained from the linearization of the infiltration rate curve (measured with the  
11 microflowmeter, MF) with respect to the inverse of the square root of time (IRC) (Eq. 11). The  $C_1$   
12 and  $C_2$  terms (Eq. 7) correspond to the slope and the intercept of the regression line obtained by  
13 plotting  $q$  (Eq. 11) as a function of  $\sqrt{t}$ . This method was tested in a laboratory on different 1D and  
14 3D soil columns. The 1D experiment consisted of two clear plastic columns of 10-cm internal  
15 diameter (i.d.) and 40-cm and 12-cm height, filled with sand (80–160  $\mu\text{m}$  grain size) and 2-mm  
16 sieved loam soil, respectively. The 3D infiltration experiments were performed on a soil clear plastic  
17 column of 30-cm i.d. and 15-cm height, filled with 2-mm sieved loam soil. Loam soil came from  
18 experimental farm of the Estación Experimental de Aula Dei (CSIC) (Zaragoza, Spain). The soil  
19 columns were uniformly packed and the soil surface levelled. A microflowmeter-disc infiltrometer  
20 with the base disc (10-cm diameter) separated from the water-supply reservoir and bubble tower was  
21 used. More details of the characteristics of the disc infiltrometer and experimental set up can be found  
22 in the previous paper in this series (Moret-Fernández et al, 2012). The cumulative infiltration and  
23 infiltration rate curves were simultaneously measured using both the standard water-level drop  
24 (WLD) in the reservoir tower and the microflowmeter (MF) methods. A  $\pm 0.5$  and a  $\pm 1$  psi differential  
25 pressure transducer (PT) (Microswitch, Honeywell) ( $\pm 1\%$  accuracy), connected to a datalogger



1 (CR1000, Campbell Scientist Inc.), were used to monitor the water flow through the MF and the drop  
2 in water level in the reservoir tower, respectively. The base infiltrometer disc, which was covered  
3 with a nylon cloth of 20- $\mu$ m mesh, was placed directly on the levelled surface of the soil columns.  
4 The interval of scanning time for the two PTs was 5-second. A single pressure head of - 1.0 cm was  
5 employed at all times during the experiment. The pressure head on the soil surface was visual  
6 controlled with the water manometer installed in the disc base (Moret-Fernández et al., 2012). The  
7 infiltration measurements for the 1D experiment ran up to 25 minutes, until the soil wetting front  
8 arrived at the bottom of the soil column. The initial and final soil volumetric water content in the 3D  
9 column was measured with a capacitive probe (Delta T, ML2x model). These experiments were  
10 repeated twice for both the sand and the 2-mm sieved loam soil. The accuracy of the IRC technique  
11 for estimating  $S_0$  and  $K_0$  was compared with the Vandervaere et al. (2000) procedure, in which the  
12 hydraulic properties are calculated from the linearization of the differential cumulative infiltration  
13 curve with respect to the square root of time (DCI) (Eq. 12). In this case, the  $C_1$  and  $C_2$  parameters  
14 (Eq. 7) are the intercept and the slope for the regression lines calculated by plotting the  $\frac{dI}{d\sqrt{t}}$  term  
15 (Eq. 12) as a function of  $\sqrt{t}$ . The coefficient of determination ( $R^2$ ) and the significance ( $p$ ) of the  
16 linearized regression models calculated using the IRC method were compared with those obtained  
17 with the DCI technique. The cumulative infiltration curves used in the DCI technique corresponded  
18 to those measured with the WLD method. These analyses were repeated on smoothed cumulative  
19 infiltration and infiltration rate data. To this end, a simple moving average algorithm

$$20 \quad \bar{y}_k = \frac{(y_{k-1} + y_k + y_{k+1})}{3} \quad (13)$$

21 was used, where  $\bar{y}_k$  is the "smoothed point" calculated from three consecutive points of the raw data  
22 ( $y_{k-1}$ ,  $y_k$  and  $y_{k+1}$ ).

1 Finally, the cumulative infiltration curves measured by the WLD method, for an infiltration time  
2 from  $t = 0$  to the wetting front reaches the bottom of the soil column, were compared with the  
3 corresponding 1D and 3D modelled functions (Eqs. 3 and 4) (Latorre, 2011) for the  $K_0$  and  $S_0$  values  
4 calculated with the DCI and IRC methods,

## 6 2.2. Field experiments

7 The IRC method was validated, using the same microflowmeter-disc infiltrometer, on three pairs  
8 of field infiltration measurements. The first pair of measurements was performed on the surface crust  
9 of a 40-cm depth loam soil (C). Two additional pairs of infiltration experiments were conducted on  
10 two different soils after removing the surface crust (at 1-cm depth): (i) a structured loam soil of a  
11 seedbed several months after a pass with a rototiller and several rainfalls (SB), and (ii) a structured  
12 loam soil several months after a pass with mouldboard plough tillage and several rainfalls (MP).  
13 More details of the soil characteristics can be found in Table 1 of the previous paper of this series  
14 (Moret-Fernández et al., 2012). All infiltration measurements were performed on a nearly level area.  
15 The base of the infiltrometer disc was covered with a nylon cloth of 20- $\mu\text{m}$  mesh and, in order to  
16 ensure good contact between the disc and the soil, a thin layer ( $< 1$  cm thickness) of commercial sand  
17 (80–160  $\mu\text{m}$  grain size) was poured onto the soil surface. The pressure head applied on the soil  
18 surface was -1.0 cm, and all infiltration measurements ran up to 10 min. As in the laboratory  
19 experiment, the accuracy of the IRC method for estimating  $S_0$  and  $K_0$ , as expressed by the calculated  
20  $R^2$  and  $p$ , was compared with the DCI technique. In these cases, the smoothed data were chosen when  
21 the  $R^2$  of the linearized regression model for the original data was lower than 0.5 (Moret-Fernández et  
22 al., 2012). In a last step, the cumulative infiltration curves measured from the drop in the reservoir  
23 water level were compared with the corresponding 3D modelled function (Eq. 4) (Latorre, 2011) for  
24 the  $K_0$  and  $S_0$  values calculated by the DCI and IRC methods.

### 1 3. RESULTS AND DISCUSSION

#### 2 3.1. Column experiments

3 The infiltration time considered in the DCI and IRC methods for all the soil-column experiments in  
4 the laboratory run between 5 to 15 and 120 to 180 s. The omission of the first few infiltration steps is  
5 justified because the relatively large time interval (5 s) used in the PT time scanning prevented the  
6 accurate estimation of infiltration values during the first few steps of the experiments, when  
7 infiltration rates were very high. These high infiltration rates resulted in some over- and  
8 underestimations of the  $\frac{dI}{d\sqrt{t}}$  and  $q$  values, respectively. The stopping time chosen for the analysis of  
9 the linearized infiltration curves is fixed by the Haverkamp et al. (1994) model, which is only valid  
10 for short to medium infiltration times.

11 The  $R^2$  and  $p$  values for the corresponding linearized regression models obtained with both the DCI  
12 (Eq. 12) and IRC (Eq. 11) methods decrease with decreasing infiltration rates (Table 1). This can be  
13 attributed to the 5 s time scanning used in the experiments, which proved to be excessively long at  
14 low infiltration rates. Smoothing the data allowed the dispersion of points to be reduced, with the  
15 corresponding improvements in the  $R^2$  and  $p$  values (Table 1). Comparison between the DCI and IRC  
16 methods applied to the 1D sand and 2-mm sieved soil columns for both the original and the smoothed  
17 data (Figs. 1 and 2) shows that the DCI procedure is more inaccurate than the IRC technique in  
18 calculating  $C_1$  and  $C_2$  (Eq. 11). Statistical analysis demonstrates that for all 1D and 3D soil columns  
19 the IRC method presents higher  $R^2$  and lower  $p$  values for the linearized regression models (Table 1),  
20 which indicates that this method is more consistent than the DCI method. As described in the  
21 previous paper in this series (Moret-Fernández et al., 2012), these differences should be attributed to  
22 the fact that the MF method allows continuous infiltration measurements, which results in more  
23 stable infiltration rate curves. On average, the standard error for the  $S_0$  and  $K_0$  parameters calculated  
24 with the DCI method for all laboratory experiments was significantly ( $p < 0.001$ ) higher (73% and

1 87% for  $S_0$  and  $K_0$ , respectively) than those obtained using the IRC technique, respectively (Table 2).  
2 These results indicate that the IRC method is more robust than the DCI model to estimate the soil  
3 hydraulic parameters.

4 Comparison between the cumulative infiltration curves measured by the WLD method and the  
5 corresponding 1D (Eq. 3) and 3D (Eq. 4) modelled function for the  $K_0$  and  $S_0$  values (Table 2)  
6 calculated with the DCI and IRC techniques (Fig. 3) shows that the IRC procedure allows better  
7 fittings between measured and modelled cumulative infiltration curves (Fig. 3). The negative  $K_0$   
8 values obtained by the DCI method in the 2-mm loam soil (Table 2) prevent the corresponding  
9 cumulative infiltration curve from being modelled (Fig. 3b). The lower RMSE values for the  
10 comparisons between all measured and modelled 1D (Eq. 3) and 3D (Eq. 4) cumulative infiltration  
11 curves verifies that the IRC method allows a better characterization of infiltration curves than the  
12 DCI technique (Table 2). Overall, no important differences were observed between the original and  
13 smoothed data when the IRC method was used (Table 2). These results suggest that for estimating  
14 soil hydraulic properties by means of the IRC technique original data would be preferable except  
15 when the  $R^2$  values of the linearized regression models are too small (e.g. the first replication of the  
16 3-D soil column experiment). In these cases, the smoothed data allow more accurate estimations of  
17  $K_0$  and  $S_0$ .

18

### 19 *3.2. Field experiments*

20 Analysis of the infiltration field experiments shows that the IRC technique allows the effect of the  
21 sand contact layer on the infiltration rate curve to be detected satisfactorily (Fig. 4). The inflection  
22 point observed in the infiltration rate curves at the beginning of the experiments indicates that a  
23 highly permeable sand layer is placed between the disc and the soil surface. Like the Vandervaere et  
24 al. (2000) procedure, the IRC method makes it possible to reveal and eliminate, in the first steps of  
25 the infiltration experiments, the influence of a sand contact layer that can lead to severe errors in

1 estimating the soil hydraulic parameters. The higher dispersion of points observed in the DCI  
2 linearized regression model (Fig. 5) indicates that the IRC method is more robust than the  
3 Vandervaere et al. (2000) technique. Overall, the linearized regression model obtained by the DCI  
4 method is less significant and with lower  $R^2$  values (Table 3). Similarly to the laboratory experiments,  
5 the standard error (SE) for the  $S_0$  and  $K_0$  parameters calculated with the IRC method (average SE  
6 values of 0.073 and 0.013 for  $S_0$  and  $K_0$ , respectively) was significantly lower ( $p < 0.1$  and  $p < 0.001$   
7 for  $S_0$  and  $K_0$ , respectively) than those obtained with the DCI technique (average SE values of 0.425  
8 and 0.306 for  $S_0$  and  $K_0$ , respectively) (Table 3). Comparison between the cumulative infiltration  
9 curves measured in the field experiments by the WLD method and the corresponding 3D modelled  
10 functions (Eq. 3) obtained for the  $K_0$  and  $S_0$  values calculated with the DCI and IRC procedures  
11 (Table 1) shows that the IRC technique allows better estimations of the cumulative infiltration  
12 curves. Further, comparison between measured and IRC modelled cumulative infiltration curves  
13 allows the effect of the sand layer on the cumulative infiltration curve to be displayed. As shown in  
14 Fig. 6, the initial volume of water stored in the sand at the beginning of the experiments causes the  
15 measured curves to jump above the modelled ones.

16

#### 17 **4. CONCLUSIONS**

18 This paper presents a new procedure for analysing infiltration curves, which, using the  
19 microflowmeter-disc infiltrometer design described in the previous paper in this series, allows soil  
20 hydraulic properties to be estimated from the linearization of the infiltration rate curve with respect to  
21 the inverse of the square root of time (IRC). This method was tested in laboratory and field  
22 experiments and compared with the Vandervaere et al. (2000) technique (DCI), which calculates the  
23 hydraulic properties from the linearization of the differential cumulative infiltration curve with  
24 respect to the square root of time (DCI). The results show that the IRC method, with higher values of  
25  $R^2$  in the linearized regression models, was considerably more robust than the DCI technique. Like

1 the DCI method, the IRC procedure makes it possible to reveal and eliminate, at the beginning of  
2 experiments, the influence of the sand contact layer that may lead to errors in estimations of the soil  
3 hydraulic parameters. Comparison between the measured and the modelled cumulative infiltration  
4 curves for the  $K_0$  and  $S_0$  values estimated with the DCI and IRC methods in both laboratory and field  
5 experiments shows that the IRC technique makes better fittings possible between measured and  
6 modelled curves. Although the DCI model could be indistinctly applied to the MF and the WLD  
7 method commonly used in the classical disc infiltrometer designs, the results show that the IRC  
8 model applied to the MF method allows the best estimations (with the lowest SD) of soil hydraulic  
9 properties. This paper offers an alternative and accurate method of estimating the soil hydraulic  
10 parameters from the analysis of the transient infiltration rate curve measured with the disc  
11 infiltrometer design described in the previous paper of this series (Moret-Fernández et al., 2012).  
12 However, new studies should be done to compare the IRC ad DCI methods to alternative  
13 linearization models (i.e. Valiantzas, 2010) and to optimize the smoothing method in order to better  
14 estimate the soil hydraulic properties. Alternatively, further efforts should be made to apply this  
15 technique to alternative infiltration instruments, such as the hood infiltrometers. To this end, a new  
16 system for fast filling up the hood base should be developed.

17

## 18 **Acknowledgements**

19 This research was supported by the Ministerio de Ciencia e Innovación of Spain (grant AGL2010-  
20 22050-C03-02).

21

## 22 **REFERENCES**

23 Angulo-Jaramillo, R., Vandervaere, J.P., Roulier, S., Thony, J.L., Gaudet, J.P., Vauclin, M., 2000.  
24 Field measurement of soil surface hydraulic properties by disc and ring infiltrometers. A  
25 review and recent developments. Soil Tillage. Research 55, 1–29.

1 Ankeny, M.D., Kaspar, T.C., Horton, R., 1988. Design for an automated tension infiltrometer. Soil  
2 Science Society of America Journal 52, 893–896.

3 Ankeny, M.D., Ahmed, M., Kaspar, T.C., Horton, R., 1991. Simple field method determining  
4 unsaturated hydraulic conductivity. Soil Science Society of America Journal 55, 467-470.

5 Casey, F.X.M., Derby, N.E., 2002. Improved design for an automated tension infiltrometer. Soil  
6 Science Society of America Journal 66, 64–67.

7 Haverkamp, R., Ross, P.J., Smettem, K.R.J., Parlange, J.Y., 1994. Three dimensional analysis of  
8 infiltration from the disc infiltrometer. Part 2. Physically based infiltration equation. Water  
9 Resources Research 30, 2931-2935.

10 Logsdon, S.D., Jaynes, D.B., 1993. Methodology for determining hydraulic conductivity with tension  
11 infiltrometers. Soil Science Society of America Journal 57, 1426-1431.

12 Latorre, B., 2011. CIC – Plotting application for 1D and 3D soil water cumulative infiltration curves.  
13 <https://apps.eead.csic.es/EEAD/apps/sueloyagua/fslc/infiltration/index.html>.

14 Moret, D., López, M.V., Arrúe, J.L., 2004. TDR application for automated water level measurement  
15 from Mariotte reservoirs in tension disc infiltrometers. Journal of Hydrology 297, 229-235.

16 Moret-Fernández, D., González, C., 2009. New method for monitoring soil water infiltration rates  
17 applied to a disc infiltrometer. Journal of Hydrology 379, 315-322.

18 Moret-Fernández, D., González, C., Lampurlanés, J., Vicente, J., 2011. An automated disc  
19 infiltrometer for infiltration rate measurements using a microflowmeter. Hydrological  
20 processes. Hydrological Processes, DOI: 10.1002/hyp.8184.

21 Moret-Fernández, D., González, C., Latorre, B. 2012. New design of microflowmeter-tension disc  
22 infiltrometer: I. Measurement of the transient infiltration rate. Journal of Hydrology (under  
23 review).

24 Parlange, Y.P., Lisle, I., Braddock, R.D., Smith, R.E., 1982. The three-parameter infiltration  
25 equation. Soil Science 133, 337-341.

1 Perroux, K.M., White, I., 1988. Designs for disc permeameters. Soil Science Society of America  
2 Journal 52, 1205–1215.

3 Philip, J.R., 1957. The theory of infiltration: 4. Sorptivity and algebraic infiltration equations. Soil  
4 Science 84, 257–264

5 Reynolds, W.D., Elrick, D.E., 1991. Determination of hydraulic conductivity using a tension  
6 infiltrometer. Soil Science Society of America Journal 55, 633–639.

7 Simunek, J., van Genuchten, M.Th., 1996. Estimating unsaturated soil hydraulic properties from  
8 tension disc infiltrometer data by numerical inversion. Water Resources Research 32, 2683–  
9 2696.

10 Simunek, J., van Genuchten, M.Th., 1997. Parameter estimation of soil hydraulic properties from  
11 multiple tension disc infiltrometer data. Soil Science 162:383–398.

12 Smettem, K.R.J., Clothier, B.E., 1989. Measuring unsaturated sorptivity and hydraulic conductivity  
13 using multi-disc permeameters. Journal of Soil Science 40, 563-568.

14 Smettem, K.R.J., Parlange, J.Y., Ross, P.J., Haverkamp, R., 1994. Three-dimensional analysis of  
15 infiltration from the disc infiltrometer. Part 1. A capillary-based theory. Water Resources  
16 Research 30, 2925-2929.

17 Turner, N.C., Parlange, J.Y., 1974. Lateral movement at the periphery of a one-dimensional flow of  
18 water. Soil Science 118, 70-77.

19 Valiantzas JD. 2010. New linearized two-parameter infiltration equation for direct determination of  
20 conductivity and sorptivity. Journal of Hydrology 384, 1-13.

21 Vandervaere, J.P., Vauclin, M., Elrick, D.E., 2000. Transient Flow from Tension Infiltrometers. Part  
22 1. The two-parameter Equation. Soil Science Society of America Journal 64, 1263-1272.

23 Warrick, A.W., Broadbridge, P., 1992. Sorptivity and macroscopic capillary length relationships.  
24 Water Resources Research 28, 427-431.



- 1 Warrick, A.W., Lomen, D.O., 1976. Time-dependent linearized infiltration: III. Strip and disc  
2 sources. *Soil Science Society of America Journal* 40, 639–643.
- 3 White, I., Sully, M.J., Perroux, K.M., 1992. Measurement of surface-soil hydraulic properties: disc  
4 permeameters, tension infiltrometers and other techniques. In: Topp, G.C., et al. (Eds.),  
5 *Advances in Measurement of Soil Physical Properties: Bringing Theory into Practice*. Soil Sci.  
6 Soc. Am. Spec. Publ. 30. SSSA, Madisson, WI, pp. 69-103.
- 7 Wooding, R.A., 1968. Steady infiltration from a shallow circular pond. *Water Resources Research* 4,  
8 1259-1273.
- 9

## FIGURE CAPTIONS

1

2

3 **Figure 1.** (a) Linearization of the differential cumulative infiltration curve with respect to the square  
4 root of time (DCI) (Eq. 12) measured from the water-level drop in the reservoir tower, and (b)  
5 linearization of the infiltration rate curve with respect to the inverse of the square root of time (IRC)  
6 (Eq. 11) obtained with the microflowmeter method, measured in the first replication of the 1D sand  
7 column experiment. White and grey circles denote the original and smoothed infiltration data,  
8 respectively.

9

10 **Figure 2.** (a) Linearization of the differential cumulative infiltration curve with respect to the square  
11 root of time (DCI) (Eq. 12) measured from the water-level drop in the reservoir tower, and (b)  
12 linearization of the infiltration rate curve with respect to the inverse of the root square of time (IRC)  
13 (Eq. 11) obtained with the microflowmeter method, measured in the first replication of the 1D 2-mm  
14 sieved loam soil column experiment. White and grey circles denote the original and smoothed  
15 infiltration data, respectively.

16

17 **Figure 3.** Comparison between the cumulative infiltration curves measured in the laboratory by the  
18 water-level drop method (circles) and the corresponding modelled (lines) functions (Eq. 3) obtained  
19 for the  $K_0$  and  $S_0$  values calculated with the DCI and IRC procedures (Table 1) from original (Or) and  
20 smoothed (Smooth) data for the first replications of (a) the 1D sand column, and (b) the 1D and (c)  
21 3D 2-mm loam soil columns.

22

23 **Figure 4.** Linearization of the infiltration rate curve with respect to the inverse of the square root of  
24 time (IRC) (Eq. 11) measured by the microflowmeter method on the second replication with the

1 structured loam soil of a seedbed several months after a pass with a rototiller for (a) original and (b)  
2 smoothed data.

3

4 **Figure 5.** DCI technique (Eq. 12) for smoothed data calculated from the cumulative infiltration  
5 curves measured with the water-level drop method (white points), and IRC technique for smoothed  
6 data calculated from the infiltration rate curves measured with the microflowmeter procedure (grey  
7 points), on the first replication with the structured loam soil of a seedbed several months after a pass  
8 with a rototiller (SB), the first replication with the structured loam soil several months after a pass  
9 with a mouldboard plough (MP), and the second replication with the crust surface of a loam soil (C).

10

11 **Figure 6.** Comparison between the cumulative infiltration curves measured from the water-level drop  
12 in the reservoir tower (circles) and the corresponding 3D modelled functions (Eq. 4) obtained for the  
13  $K_0$  and  $S_0$  values calculated with the DCI (dashed line) and IRC (solid line) procedures (Table 1) on  
14 (a) the second replication with the structured loam soil of a seedbed several months after a pass with  
15 a rototiller, (b) the second replication with the structured loam soil several months after a pass with a  
16 mouldboard plough, and (c) the first replication with the crust surface of a loam soil.

17

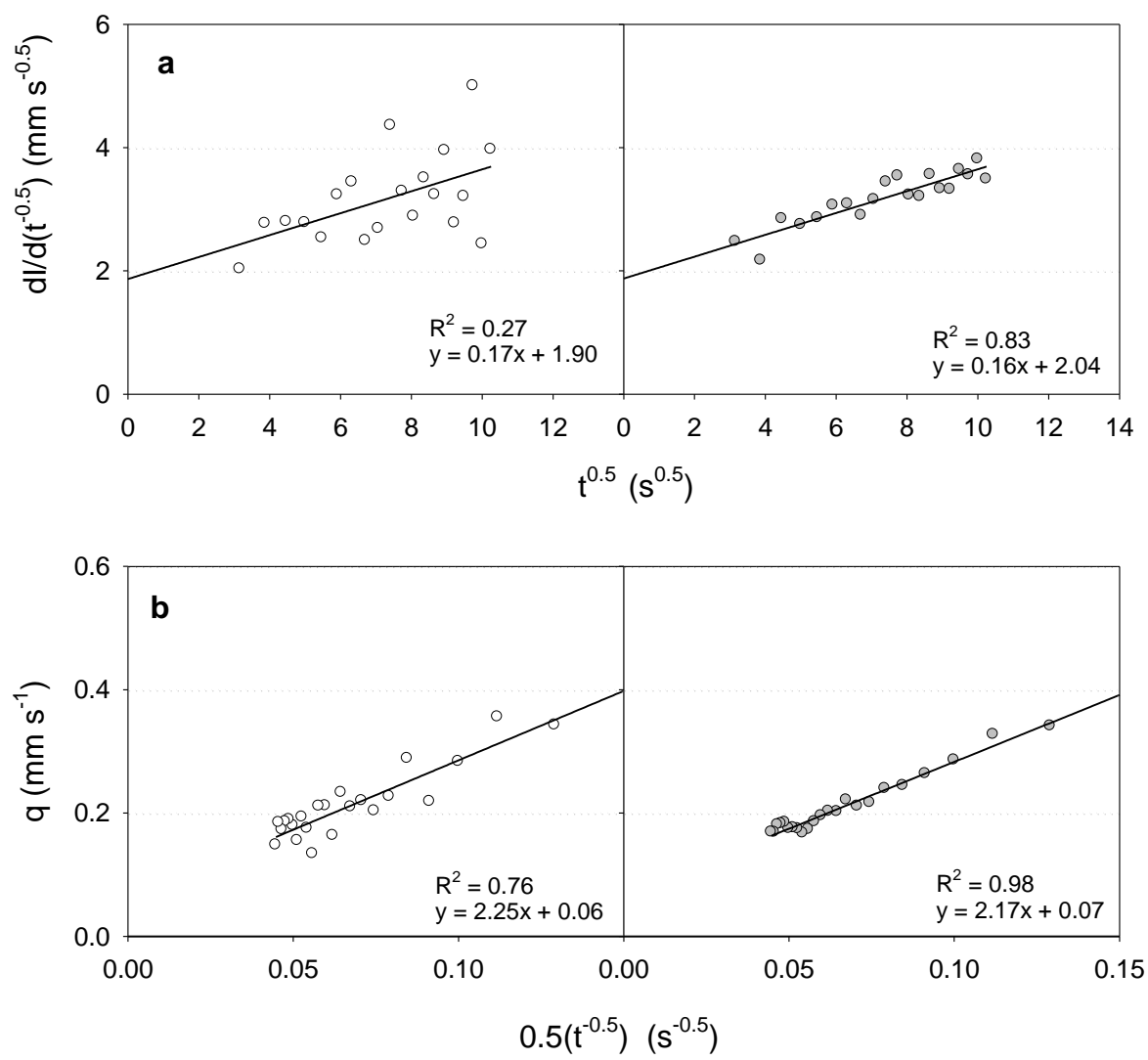


Figure 1.

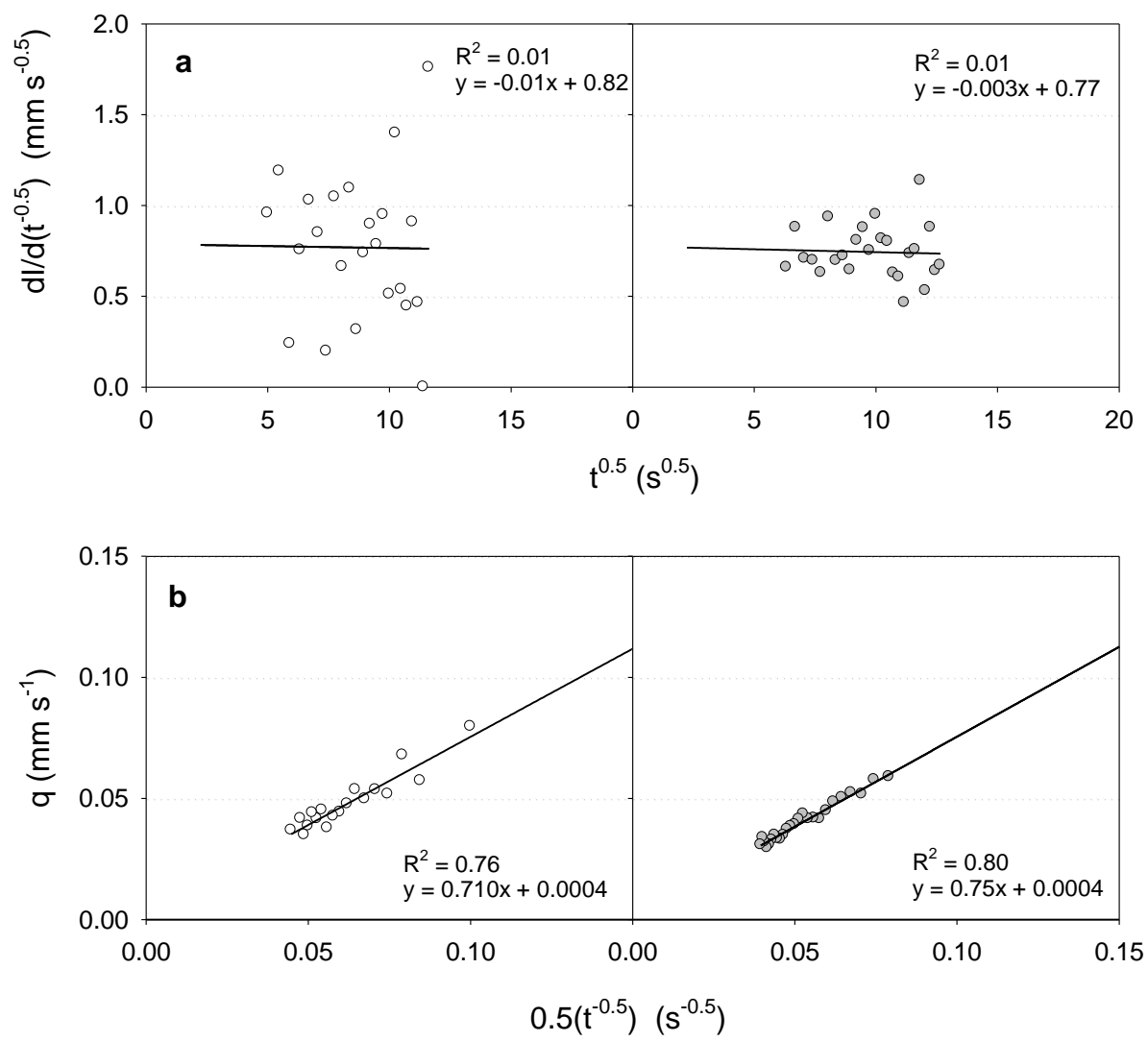


Figure 2.

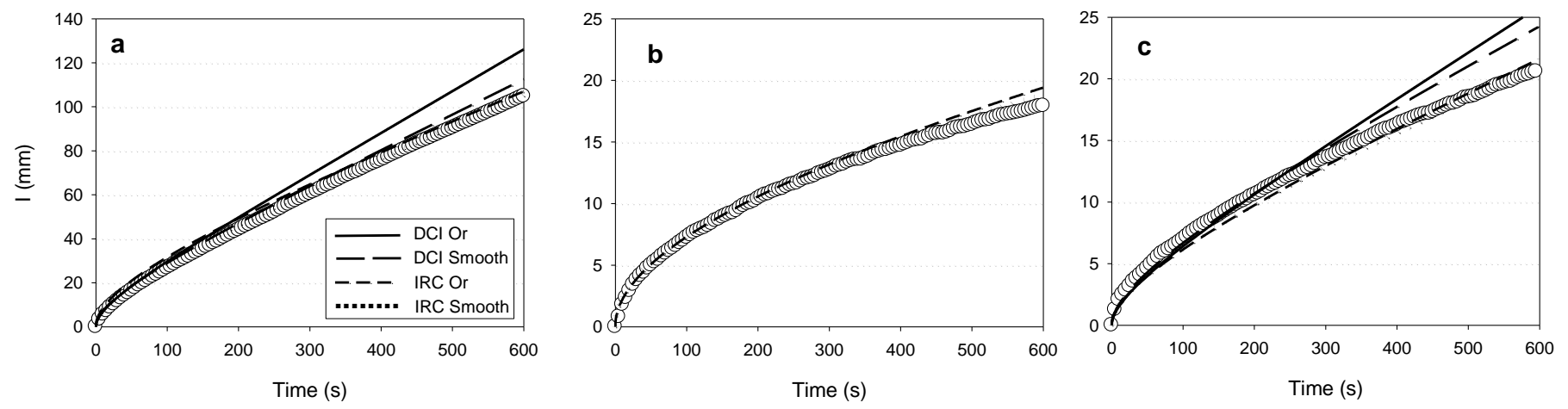


Figure 3

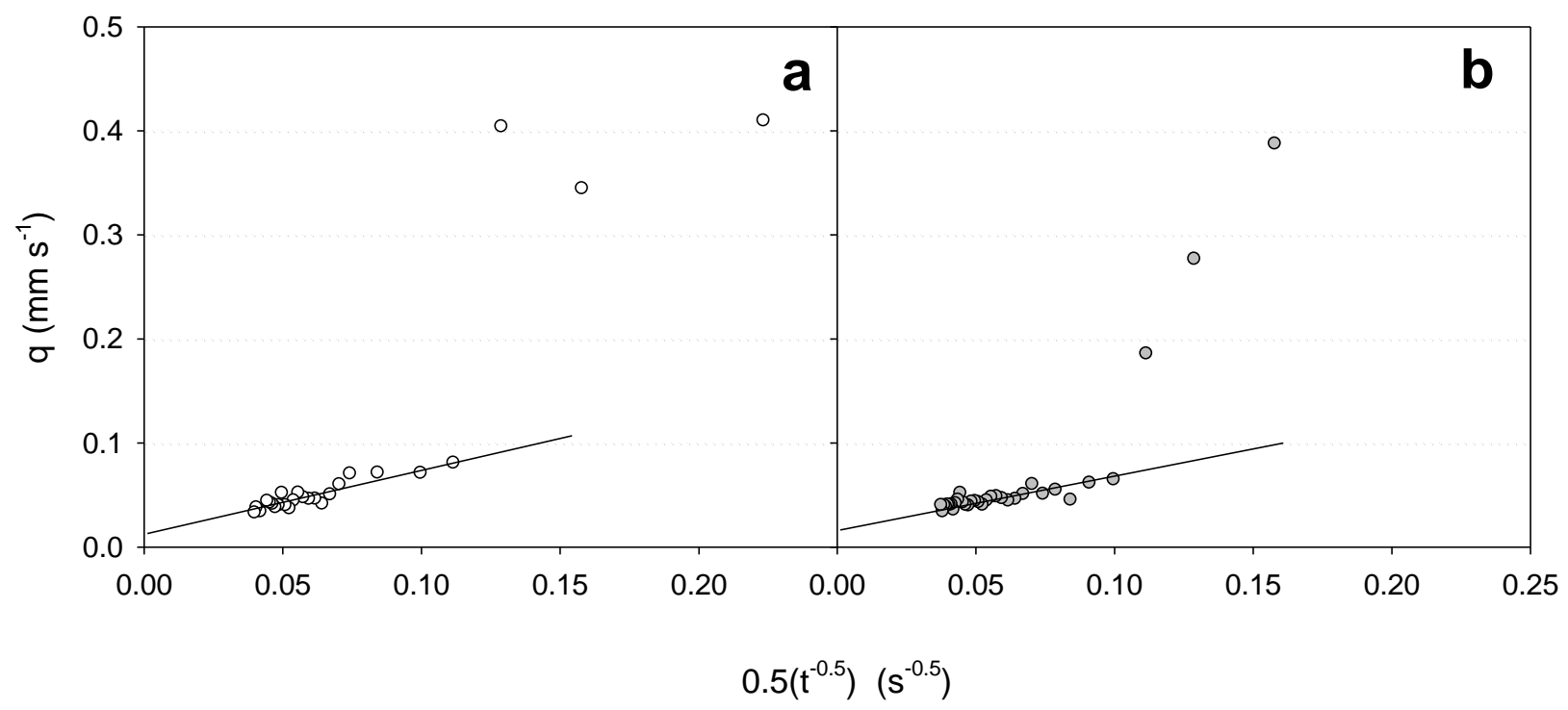


Figure 4.

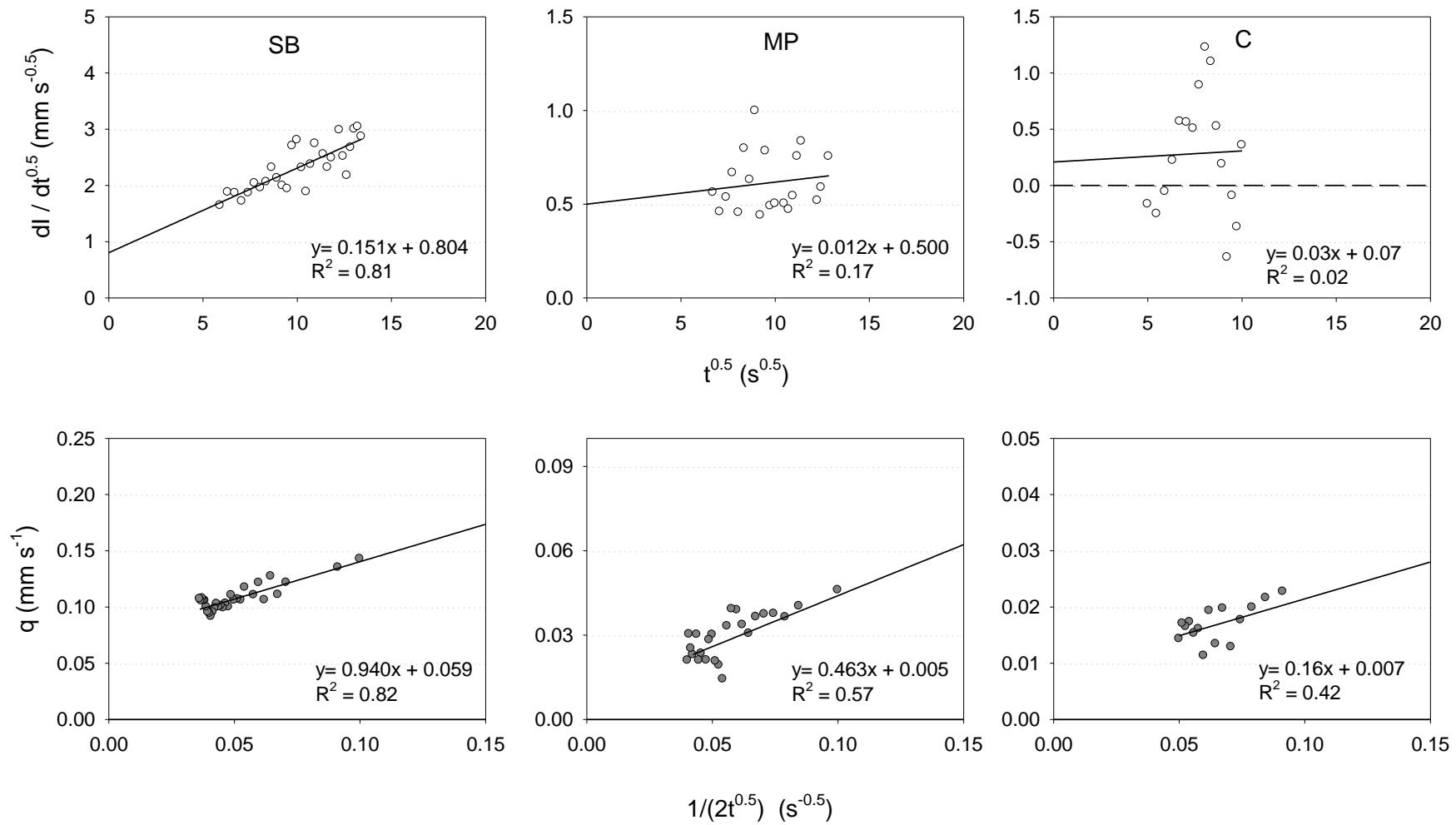


Figure 5.



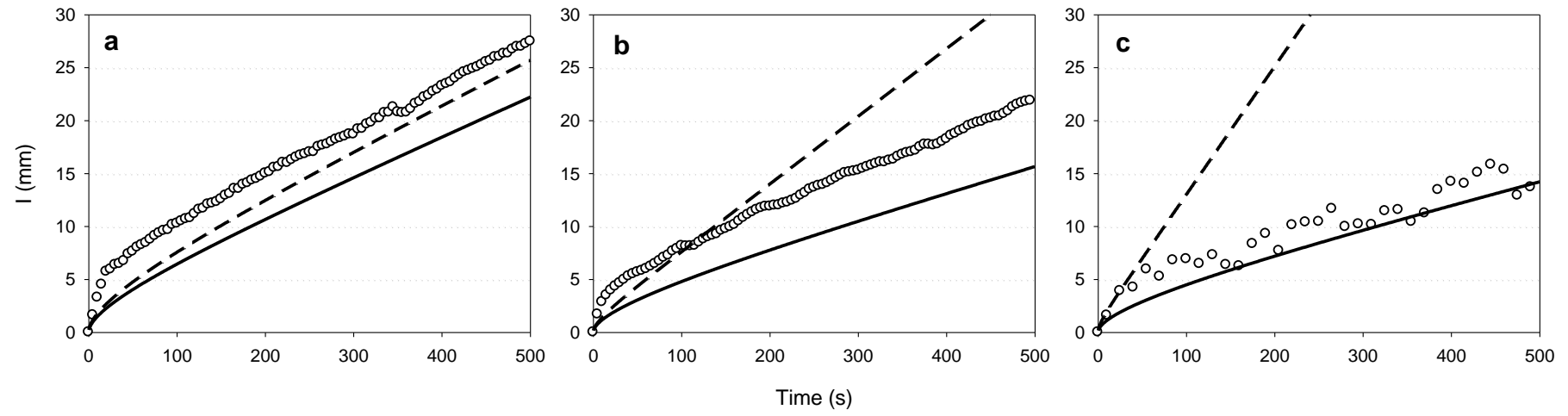


Figure 6.

**Table 1.** Coefficient of determination ( $R^2$ ), slope and intercept (S&I) and significance ( $p$ ) of the linearized regression models, for all 1D and 3D soil columns after applying the DCI and IRC methods on the original (Or) and smoothed (Sm) infiltration curves measured in sand and 2-mm sieved loam soil (Loam).

Column	Soil	Repl	Analysis	Data	$R^2$	S&I	$p$	
1D	Sand	1	DCI	Or	0.27	$y = 0.17x + 1.90$	0.009	
				Sm	0.83	$y = 0.16x + 2.04$	<0.001	
		2		Or	0.15	$y = 0.29x + 3.08$	0.12	
				Sm	0.51	$y = 0.21x + 3.62$	<0.001	
	Loam	1		Or	0.01	$y = -0.01x + 0.82$	0.88	
				Sm	0.01	$y = -0.03x + 0.77$	0.85	
		2		Or	0.05	$y = 0.018x + 0.17$	0.30	
				Sm	0.20	$y = 0.017x + 0.18$	0.04	
3D	Loam	1	Or	0.35	$y = 0.05x + 0.29$	0.45		
			Sm	0.13	$y = 0.03x + 0.39$	0.11		
		2	Or	0.15	$y = 0.04x + 0.41$	0.11		
			Sm	0.39	$y = 0.38x + 0.46$	0.001		
	1D	Sand	1	IRC	Or	0.76	$y = 2.25x + 0.064$	<0.001
					Sm	0.98	$y = 2.17x + 0.07$	<0.001
			2		Or	0.91	$y = 3.64x + 0.097$	<0.001
					Sm	0.95	$y = 3.82x + 0.082$	<0.001
Loam		1	Or		0.76	$y = 0.71x + 0.004$	<0.001	
			Sm		0.80	$y = 0.75x + 7.1E-4$	<0.001	
		2	Or		0.56	$y = 0.35x + 0.0008$	<0.001	
			Sm		0.69	$y = 0.34x + 0.002$	<0.001	
3D	Loam	1	Or	0.29	$y = 0.37x + 0.013$	0.005		
			Sm	0.68	$y = 0.33x + 0.012$	<0.001		
	2	Or	0.79	$y = 0.44x + 0.016$	<0.001			
		Sm	0.74	$y = 0.48x + 0.014$	<0.001			

**Table 2.** Root mean square error (RMSE) for the comparison between the cumulative infiltration curves (from 0 to 600 s) measured from the water-level drop in the water reservoir and the corresponding 1D (Eq. 3) and 3D (Eq. 4) modelled function for the  $K_0$  and  $S_0$  values calculated with the DCI and IRC methods (Table 1) for original (Or) and smoothed (Sm) infiltration curves on the 1D sand and 2-mm sieved loam soil and 3D 2-mm sieved loam soil columns.  $SE_{S_0}$  and  $SE_{K_0}$  are the standard errors of the  $S_0$  and  $K_0$  parameters, respectively.

Column	Soil	Replication	Analysis method	Data	$S_0$	$SE_{S_0}$	$K_0$	$SE_{K_0}$	RMSE
					mm s <sup>-0.5</sup>		mm s <sup>-1</sup>		
1D	Sand	1	DCI	Or	1.905	0.500	0.189	0.131	11.90
				Sm	2.041	0.135	0.162	0.036	4.33
		2	Or	3.081	1.375	0.308	0.373	25.08	
			Sm	3.623	0.406	0.227	0.096	9.96	
	Loam soil	1	Or	0.819	0.399	-0.064	0.964	-	
			Sm	0.768	0.160	-0.003	0.343	-	
		2	Or	0.171	0.155	0.018	0.036	1.36	
			Sm	0.179	0.059	0.017	0.015	1.20	
3D	Loam soil	1	Or	0.290	0.553	0.042	0.230	5.35	
			Sm	0.392	0.148	0.020	0.070	0.67	
		2	Or	0.415	0.229	0.030	0.090	2.35	
			Sm	0.468	0.840	0.021	0.020	1.56	
1D	Sand	1	IRC	Or	2.251	0.281	0.126	0.043	3.41
				Sm	2.170	0.084	0.145	0.015	2.49
		2	Or	3.639	0.227	0.186	0.036	1.02	
			Sm	3.826	0.155	0.176	0.026	1.25	
	Loam soil	1	Or	0.705	0.079	8.6E-3	8.6E-3	1.07	
			Sm	0.751	0.080	1.5E-3	2.1E-4	0.54	
		2	Or	0.359	0.078	1.1E-3	0.011	0.28	
			Sm	0.340	0.051	6.4E-4	6.4E-3	0.43	
3D	Loam soil	1	Or	0.368	0.119	0.017	0.026	0.86	
			Sm	0.346	0.062	0.017	0.031	1.05	
		2	Or	0.445	0.078	0.017	0.012	0.64	
			Sm	0.48	0.051	0.009	0.013	0.62	

**Table 3.** Coefficient of determination ( $R^2$ ), slope and intercept (S&I) and significance ( $p$ ) of the linearized regression models, and average and standard errors (SE) for the hydraulic conductivity ( $K_0$ ) and sorptivity ( $S_0$ ) values calculated in all field experiments with the DCI and IRC methods on original (Or) or smoothed (Sm) infiltration curves.

Soil	Replication	Analysis	Data	$R^2$	S&I	$p$	$S_0$		$K_0$	
							mm s <sup>-0.5</sup>	mm s <sup>-1</sup>		
SB <sup>a</sup>	1	DCI	Sm	0.67	$y = 0.15x + 0.81$	< 0.001	0.819	0.208	0.102	0.812
	2		Sm	0.19	$y = 0.49x + 0.48$	0.03	0.488	0.198	0.032	0.073
MP <sup>b</sup>	1		Sm	0.17	$y = 0.01x + 0.51$	0.58	0.506	0.198	-0.011	0.068
	2		Sm	0.18	$y = 0.06x + 0.34$	0.07	0.339	0.321	0.059	0.122
C <sup>c</sup>	1		Sm	0.05	$y = 0.12x + 0.40$	0.43	0.405	1.205	0.114	0.538
	2		Sm	0.02	$y = 0.03x + 0.07$	0.63	0.069	0.423	0.029	0.226
SB	1	IRC	Sm	0.82	$y = 0.94x + 0.059$	< 0.001	0.879	0.112	0.068	0.009
	2		Sm	0.89	$y = 0.41x + 0.018$	< 0.001	0.413	0.081	0.030	0.015
MP	1		Sm	0.57	$y = 0.33x + 0.014$	< 0.001	0.326	0.051	0.021	0.010
	2		Sm	0.39	$y = 0.35x + 0.013$	0.001	0.333	0.081	0.020	0.017
C	1		Sm	0.57	$y = 0.32x + 0.012$	< 0.001	0.319	0.067	0.017	0.017
	2		Sm	0.42	$y = 0.16x + 6.6E-3$	0.009	0.151	0.049	0.013	0.011

<sup>a</sup> Structured loam soil of a seedbed several months after a pass with a rototiller

<sup>b</sup> Structured loam soil several months after a pass with mouldboard plough tillage

<sup>c</sup> Crust surface of a loam soil